

# Catalysis Science & Technology

Accepted Manuscript



This article can be cited before page numbers have been issued, to do this please use: L. Vilcoq, V. Spínola, P. Moniz, L. Duarte, F. Carvalho, C. E. Fernandes and P. Castilho, *Catal. Sci. Technol.*, 2015, DOI: 10.1039/C5CY00195A.



This is an *Accepted Manuscript*, which has been through the Royal Society of Chemistry peer review process and has been accepted for publication.

*Accepted Manuscripts* are published online shortly after acceptance, before technical editing, formatting and proof reading. Using this free service, authors can make their results available to the community, in citable form, before we publish the edited article. We will replace this *Accepted Manuscript* with the edited and formatted *Advance Article* as soon as it is available.

You can find more information about *Accepted Manuscripts* in the [Information for Authors](#).

Please note that technical editing may introduce minor changes to the text and/or graphics, which may alter content. The journal's standard [Terms & Conditions](#) and the [Ethical guidelines](#) still apply. In no event shall the Royal Society of Chemistry be held responsible for any errors or omissions in this *Accepted Manuscript* or any consequences arising from the use of any information it contains.



## Catalysis Science &amp; Technology

## ARTICLE

## Acid-modified clays as green catalysts for the hydrolysis of hemicellulosic oligosaccharides

Léa Vilcoq,<sup>a</sup> Vitor Spinola,<sup>a</sup> Patricia Moniz,<sup>b</sup> Luís C. Duarte,<sup>b</sup> Florbela Carvalheiro,<sup>b</sup> César Fernandes<sup>a,c</sup> and Paula Castilho<sup>\*a</sup>Received 00th January 20xx,  
Accepted 00th January 20xx

DOI: 10.1039/x0xx00000x

www.rsc.org/

The hydrolysis of hemicellulosic oligosaccharides (OS) was investigated using acid-activated clays (prepared from natural Porto Santo montmorillonite clay), as catalysts. Acid activation was performed in HCl solution or with aluminium exchange. The clay catalysts were characterized by XRD, N<sub>2</sub> adsorption isotherms, CEC, FTIR, titration of acid sites in water and adsorption of sugars and disaccharides. They were tested for the hydrolysis of a model compound, maltose, and of oligosaccharide (OS)-rich liquor from rice straw fractionation. The HCl-activated clays were the most efficient catalysts for maltose hydrolysis. It was demonstrated that the hydrolysis of OS into monomer sugars over a clay catalyst is technically feasible and that this reaction leads to the selective removal of glucose, arabinose and acetic acid side-groups from the OS structure, thus yielding to simpler xylo-oligosaccharide chains. Furthermore, no significant conversion of monomer sugars into furans was observed.

## 1. Introduction

Hemicelluloses are one of the three main components of lignocellulosic biomass, together with cellulose and lignin, representing from 15 to 35 wt.% of biomass dry weight, and its upgrade is considered today as an essential element of cost-effectiveness for biorefinery processes.<sup>1</sup> It contains several sugars, namely pentoses (such as xylose, arabinose), and hexoses (such as glucose, galactose and mannose).<sup>2</sup> The most abundant hemicelluloses, especially in angiosperms, are xylans, where xylose units constitute the skeleton of the hemicellulose chain, with glucose, arabinose, galactose and/or mannose as side units. Acetyl groups and uronic acids are also typically present.

To upgrade hemicelluloses, their separation from cellulose and lignin is required and various pre-treatment methods, such as dilute acid hydrolysis, autohydrolysis or steam explosion, have been developed.<sup>3, 4</sup> These processes lead to deconstruct lignocellulose into a solid fraction, containing mainly cellulose and lignin, and an aqueous liquid fraction,

containing ex-hemicellulose sugars, acetic acid and some impurities. Depending on the operating conditions, a large amount of these sugars is usually in the oligomeric form. Although these oligosaccharides (OS) can be marketable by themselves, their low market volume imposes the use of other alternatives. As such, further hydrolysis into monomeric sugars, mainly xylose, arabinose and glucose will enable their final transformation by fermentation or chemical catalysis into biofuels (e.g. bioethanol or biobutanol) or bioproducts (e.g. xylitol, furfural, etc.).<sup>2, 5-7</sup> Hemicellulosic OS are currently hydrolysed with mineral acids such as sulphuric acid,<sup>4</sup> leading to the dehydration of a part of the produced sugars into furfural and 5-hydroxymethylfurfural (HMF) and to safety and corrosion issues. OS can also be hydrolyzed by enzymes, but the process is more expensive, requires long reaction times and the action of several accessory enzymes, and the yields are rather low when compared with those obtained by acid hydrolysis. A green alternative is the replacement of mineral acids by solid acid catalysts during OS hydrolysis, with increased sugars selectivity.

Hemicellulose or hemicellulosic OS hydrolysis using solid acid catalysts aroused less interest than cellulose hydrolysis in literature (for a review see <sup>8</sup>). Sulfonated resins<sup>9</sup> and sulfonated silica<sup>10</sup> have been used for this purpose. Zeolites, resins, activated carbons and functionalized oxides are also able to hydrolyse model disaccharides compounds (sucrose and cellobiose).<sup>11</sup> Among these catalysts, those with a high hydrophilic surface (e.g. carbon materials) with a good adsorption capacity for polar compounds, such as sugars and OS, are very efficient.<sup>12</sup>

Montmorillonite clays are natural layered materials which can be found for example on Porto Santo Island in Madeira

<sup>a</sup> Centro de Química da Madeira (CQM), Centro de Ciências Exatas e da Engenharia da Universidade da Madeira, Campus Universitário da Penteada, 9000-390 Funchal, Portugal. Fax: +351 291 705 149; Tel: +351 291 705 102. e-mail: vilcoq@uma.pt; vitorspinola@uma.pt; castilho@uma.pt.

<sup>b</sup> Unidade de Bioenergia, LNEG (Laboratório Nacional de Energia e Geologia), Ed. K2, Est. do Paço do Lumiar 22, 1649-038 Lisboa, Portugal. Fax: + 351 217 166 966; Tel: +351 210 924 713. e-mail: patricia.moniz@lneg.pt; florbela.carvalheiro@lneg.pt; luis.duarte@lneg.pt.

<sup>c</sup> Laboratório Regional de Engenharia Civil, Rua Agostinho Pereira de Oliveira, 9000-264 Funchal, Portugal. Fax: +351 291724061; Tel: +351 291724060. e-mail: cfernandes@lrec.pt.

Electronic Supplementary Information (ESI) available: [FTIR spectra of adsorbed pyridine over activated clays (Figure) and final carbon balances during the maltose hydrolysis test (Table)]. See DOI: 10.1039/x0xx00000x

archipelago.<sup>13</sup> Their layered structure consists in a pile 55  
tetrahedral and octahedral layers linked with oxygen bonds.  
The interlayer space contains cations and water and  
represents a very large and very polar surface area.<sup>14</sup> The clays  
5 can be modified by acid activation, *i.e.* exchanging interlayer  
cations with protons, or by cationic exchange, *e.g.* with  $\text{Al}^{3+}$   
cations.<sup>15</sup> The resulting materials can be used as solid acid  
catalysts for a wide range of reactions.<sup>16</sup> Clays have been used  
successfully for cellulose conversion<sup>17</sup> and for lignocellulose  
10 and hemicellulose hydrolysis.<sup>18,19</sup> Thus, clay catalysts could be  
a promising green and cost-effective alternative for 65  
hydrolysis.

In this paper, activated clays prepared from natural Porto  
Santo montmorillonite by acid activation with HCl solutions or  
15 by aluminium exchange are studied as catalysts for the  
hydrolysis of a model disaccharide, maltose, and for the  
hydrolysis of an oligosaccharide-containing liquor obtained  
from hydrothermal fractionation (autohydrolysis) of rice straw.  
The acidity of clays and their ability to adsorb sugars and  
20 polysaccharides are discussed. To study the clays ability to  
hydrolyse OS, four parameters were selected: i) the acidity in  
water, measured by a common method of acid-base titration;  
ii) the sugars adsorption, investigated by XRD; iii) the maltose  
hydrolysis activity and selectivity and iv) the recyclability of the  
25 catalyst.

## 2. Experimental

### 2.1. Rice straw autohydrolysis

The oligosaccharide-containing liquor was obtained by  
hydrothermal treatment (autohydrolysis) of rice straw.<sup>85</sup>  
Autohydrolysis treatment was carried out in a stainless steel  
reactor (Parr Instruments Company, USA) with a total volume  
of 2 L under previously optimized conditions.<sup>20,21</sup> Briefly, the  
raw material was mixed with water in the reactor in order to  
obtain a mass liquid-to-solid ratio of 10. The agitation speed  
35 was set at 150 rpm and the reactor heated ( $3.8^{\circ}\text{C}\cdot\text{min}^{-1}$ ) to  
reach a final temperature of  $210^{\circ}\text{C}$ , after which the reactor  
was rapidly cooled down. The liquid and solid phases were  
recovered by pressing (up to 200 bar) using a hydraulic press  
(Sotel, Portugal) and the liquid phase was further filtered  
40 (Whatman filter paper n°1).

### 2.2. Clays preparation

The purification of Porto Santo clays has already been  
described in previous publications.<sup>22</sup> Briefly, the clay was  
collected at Serra de Dentro site, on Porto Santo island in the  
Madeira archipelago, coned, quartered, and sieved to the  
45  $<0.125$  mm fraction, then the resulting representative sample  
was decarbonated with hydrogen peroxide, washed with  
deionised water, sonicated for 5 min in order to promote  
disaggregation and the  $<2$   $\mu\text{m}$  fraction was collected after 8 h  
sedimentation. The Na-exchanged form, subsequently referred  
50 to as SDN-Na, was prepared using 1 M aqueous sodium  
chloride solution. Excess  $\text{Cl}^{-}$  was removed by dialysis. Chemical  
composition data of SDN-Na indicated the presence of some  
residual calcium oxide (0.5 %), which could not be attributed

entirely to an external calcium phase. Further Na-exchange  
was achieved by mixing  $\text{Na}_{3.5}\text{EDTA}$  with the clay, stirring the  
suspension overnight and centrifuging and washing the clay  
until the supernatant reached a stable, low conductivity.

The HCl-activated clays were prepared by stirring the initial  
SDN-Na clay in HCl solution at  $95^{\circ}\text{C}$ , during 30 min, in a closed  
boiling flask. The clay was then filtrated over Whatman filter  
paper n°1, washed thoroughly with deionised water, then  
dried overnight at  $60^{\circ}\text{C}$  and ground. The clays are labelled  
SDNxM for a clay activated in x M HCl solution (x = 1, 2 or 6).

The aluminium-exchanged clay was prepared by stirring  
1 % suspension of the clay in  $0.3\text{ mol}\cdot\text{L}^{-1}$   $\text{AlCl}_3$  solution  
overnight. The suspension was then centrifuged and the  
resulting material thoroughly washed, dried overnight at  $60^{\circ}\text{C}$   
and ground. The exchanged clay is labelled SDN-Al.

### 2.3. Characterizations

X-ray diffraction (XRD) measurements were performed on a  
Bruker D8 Advance apparatus. Before analysis, the catalyst  
was crushed to a fine powder (around 100 mg of sample was  
necessary). The interlayer spacing was measured from the  
position of the peak between  $4$  and  $10^{\circ}$  2-theta, after  
background correction.

The specific surface areas were determined by nitrogen  
adsorption at  $-196^{\circ}\text{C}$  using a Micrometrics ASAP 2020  
equipment. Samples were previously degassed at  $150^{\circ}\text{C}$  under  
vacuum ( $10^{-3}$  Pa) for 5 h. Surface areas were calculated using  
the Brunauer–Emmet–Teller (BET) method.

The CEC values were determined using the method  
introduced by Ammann *et al.*<sup>23</sup> using the copper triethylene  
tetramine complex. 100 mg  $\pm$  25 mg of dry clay were weighed  
in 25 ml centrifugal tubes. 8 ml of 0.01 M complex solution  
were added. The samples were shaken for at least 30 minutes  
and then centrifuged at a relative centrifugal field of 3000 g for  
10 minutes. 3 ml of the supernatant were filled into cuvettes  
and the adsorption was measured at 577 nm. Every  
determination was carried out with three parallel samples.

The nature of acid sites was determined by pyridine  
adsorption with FTIR on a Fourier Vector 22 Bruker apparatus.  
The clay was deposited as a suspension on a germanium  
support and dried at  $120^{\circ}\text{C}$ . After vacuum treatment during 30  
min, pyridine was adsorbed on the catalyst and the cell was  
heated at  $150^{\circ}\text{C}$  during 1 h. The spectra were recorded after  
vacuum treatment during 30 min at room temperature and  
then during 30 min at  $150^{\circ}\text{C}$ . The molar ratio of Brønsted and  
Lewis sites was determined following the Beer law, according  
to methods from the literature.<sup>24,25</sup> The formula for calculating  
the molar ratio of Brønsted and Lewis sites was:

$$\text{Brønsted}/\text{Lewis} = \frac{A_{\text{Brønsted}} \times \epsilon_{\text{Lewis}}}{A_{\text{Lewis}} \times \epsilon_{\text{Brønsted}}}$$

with  $A_{\text{Brønsted}}$  the area of the B-Py band at  $1545\text{ cm}^{-1}$ ,  $A_{\text{Lewis}}$  the  
area of the L-Py band at  $1450\text{ cm}^{-1}$  and  $\epsilon$  the molar extinction  
coefficients from <sup>24</sup>.

The acid sites concentration in water of each catalyst was  
measured using a simple acid-base titration protocol:<sup>26</sup> 40 mg  
of catalyst were added to 20 mL of NaOH 0.01 M. The solution  
was stirred at room temperature during 2 h. After filtration,

the pH of the filtrate was determined by titration with HCl 0.01 M and phenolphthalein. The number of acid sites was calculated as follows:

$$N_s = \frac{([OH^-]_i - [OH^-]_{2h}) \times V}{m_{cat}}$$

with [OH<sup>-</sup>] the hydroxide molar concentration determined by titration (mol.L<sup>-1</sup>), V the solution volume (L) and m<sub>cat</sub> the mass of catalyst (g). Each experiment was duplicated. ICP-OES measurements were performed on an ACTIVA apparatus (from Jobin-Yvon).

2.4. Maltose and sugars adsorption

0.25 g of clay was added to 10 mL of a maltose or sugars solution (maltose 30 g.L<sup>-1</sup> or glucose-xylose-arabinose 10 g.L<sup>-1</sup> each) and stirred at room temperature, during 2 h. A few drops of the suspension of clay in sugars or maltose solutions were deposited on a glass blade without filtration and dried at 60°C during 2 days and then analysed by XRD.

2.5. Catalytic test

A steel tube reactor was filled with 10 mL of hydrolysate or maltose solution 10 g.L<sup>-1</sup>, the catalyst (0.25 g) and a magnetic stirrer. The reactor was then heated at 120°C using a hot plate and a silicon oil bath. The water autogenous pressure was lower than 2 bar and reaction medium remained in the liquid state. Samples were taken regularly by cooling quickly the reactor under flowing water, opening it, sampling and filtrating 0.5 mL (cellulose acetate filter, 0.45 µm) of the reaction medium. Some catalyst was removed at each sampling, but it was considered as negligible for the reaction. After 24 h, liquid and solid were separated by filtration and the catalyst was dried at 110°C in a muffle furnace.

2.6. Products analysis

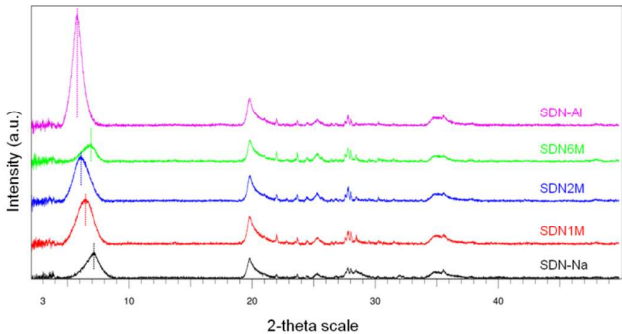
Maltose, fructose, glucose, xylose, arabinose, acetic acid, HMF and furfural were analysed by HPLC using a refractive index detector (RID), a diode array detector (DAD) whenever necessary and a Rezex RHM-Monosaccharide H<sup>+</sup> column (Phenomenex).

Post-hydrolysis assays were performed to evaluate the maximum sugars yield that could be obtained from the OS-containing liquor. This was carried out in universal Schott flasks in autoclave at 121°C, 4 % H<sub>2</sub>SO<sub>4</sub> concentration, 60 min. After 1 h, the autoclave was rapidly cooled down to 100°C (approximately 3 min). The resulting liquid was filtrated and analysed by HPLC. The contents in xylo-oligosaccharides (XOS), gluco-oligosaccharides (GlcOS), arabino-oligosaccharides (AOS) and acetyl group linked to OS (AcOS) were calculated from the concentration increase for xylose, glucose, arabinose and acetic acid after post-hydrolysis.

3. Results and discussion

3.1. Characterizations

The clays catalysts were characterized by XRD, N<sub>2</sub> adsorption, CEC measurement, pyridine adsorption followed by FTIR and NaOH titration (Table 1). Considering SDN-Na as standard, the



XRD diffractograms (Figure 1) of acid treated clays showed a shift of the d001 peak, which corresponds to the basal spacing, Figure 1. XRD diffractograms of clay catalysts.

to lower angles, indicating that the interlayer spacing increases for the SDN1M and SDN2M clays. This can be interpreted as an exchange of the interlayer Na<sup>+</sup> cation with a proton coupled with a slight leaching of the octahedral layers.<sup>14</sup> Then a slight shift to the higher angle is observed for the d001 peak in the case of SDN6M. The peak is also smaller, indicating a loss of structure, as already described in severe activation conditions.<sup>28</sup> For SDN-Al, an interlayer spacing increase occurred during the exchange Na<sup>+</sup>-Al<sup>3+</sup> in the interlayer space.

Table 1. Characterisations of the clay catalysts

Catalyst	Δd <sup>a</sup> (Å)	S <sub>BET</sub> -N <sub>2</sub> (m <sup>2</sup> .g <sup>-1</sup> )	CEC (m <sub>eq</sub> .100 g <sup>-1</sup> )	Brønsted/Lewis molar ratio <sup>b</sup>	Acid sites concentration (mmol <sub>H+</sub> .g <sub>cat</sub> <sup>-1</sup> )
SDN-Na	12.5	118	84	0,10	1.09
SDN1M	13.8	375	53	2,42	1.7
SDN2M	14.7	425	47	0,92	1.61
SDN6M	13	460	32	0,70	1.51
SDN-Al	15.4	140	55	1,36	1.79

<sup>a</sup> Interlayer spacing, from the XRD diffractogram.

<sup>b</sup> Calculated from the area of the FTIR band at 1540 cm<sup>-1</sup> (Brønsted sites) and the area of the FTIR band at 1450 cm<sup>-1</sup> (Lewis site)

The surface area measurement of clays is complex. The nitrogen adsorption-desorption following the Brunauer-Emmet-Teller method gives only the non polar surface area of porous solids.<sup>29</sup> However, an important part of the clay surface is very polar, especially the internal surface of the interlayer space. This polar surface could be as high as 700 m<sup>2</sup>.g<sup>-1</sup>, in the case of a Na-montmorillonite, analysed by methylene blue adsorption.<sup>30</sup> For SDN clay catalysts, the initial BET specific surface area (SDN-Na) is low, 118 m<sup>2</sup>.g<sup>-1</sup>. It is not drastically modified by the ion exchange with aluminium (140 m<sup>2</sup>.g<sup>-1</sup>) but drastically increases during acid activation in HCl, in correlation with the HCl concentration, giving a final specific surface area of 460 m<sup>2</sup>.g<sup>-1</sup> for SDN6M. Thus, the acid activation of SDN-Na leads to an increase in the specific surface area, as a consequence of the loss of Al<sup>3+</sup> from the octahedral sheet due to the acid treatment. The opening of pores obstructed by amorphous species, then dissolved during the acid activation,



can also be involved. When the acid concentration during activation increases the increase in specific surface area is attributed to the loss of layered structure observed by XRD, improving the accessibility of clay surface.

The cation exchange capacity (CEC) of fresh catalyst was determined (Table 1). The results are coherent with those obtained for previous studies.<sup>13</sup> The native SDN-Na clay has the higher CEC value (84 m<sub>eq</sub>·100 g<sup>-1</sup>). The acid treated clays have lower CEC, as expected, due to the partial destruction of the layer structure as already reported by Komadel.<sup>31</sup> This effect is more pronounced at high acid concentration. Theoretically, SDN-Al should give a CEC close to SDN-Na, but due to higher Al<sup>3+</sup> affinity, the CEC value is lower.

The pyridine adsorption followed by FTIR was performed at 150°C. After desorption of the physisorbed pyridine, the FTIR spectra of adsorbed pyridine showed the bands described in literature as typical of Lewis-bound pyridine (1450, 1490, 1590 and 1620 cm<sup>-1</sup>) and Brønsted acid-bound pyridinium cation bands (1540 and 1640 cm<sup>-1</sup>), except for SDN-Na which did not exhibit the 1590 cm<sup>-1</sup> and 1640 cm<sup>-1</sup> bands (ESI Figure S1). The molar ratio of Brønsted/Lewis sites was calculated from the areas of the B-Py band at 1545 cm<sup>-1</sup> and of the L-Py band at 1450 cm<sup>-1</sup>. The few acid sites present on the SDN-Na are Lewis sites in majority. For the acid-treated clays, the Brønsted/Lewis ratio is close to 1, indicating the formation of Brønsted and Lewis acid sites during the acid activation. For the SDN-Al clay, there is a majority of Brønsted sites even if the L-Py band indicates the presence of numerous Lewis acid sites.

A titration of the acid sites was performed on all the catalysts. The acid-base titration of the catalysts evidences the presence of acid sites in the presence of water (Table 1). The average concentration of acid sites is 1.7 mmol<sub>H+</sub>·g<sup>-1</sup>, a value close to what is reported for Amberlyst-15 resin (1.8 mmol<sub>H+</sub>·g<sup>-1</sup>) and sulfonated carbon (1.6 mmol<sub>H+</sub>·g<sup>-1</sup>) in the literature.<sup>26</sup> The acidity ranking of the clay catalysts is: SDN-Na < SDN6M < SDN2M < SDN1M < SDN-Al, indicating that the partial structural decomposition occurring during acid activation in harsh conditions, *i.e.* with HCl 6 M solution, does not favour the formation of active acid sites in water, contrarily to the activation in mild conditions (SDN1M). This result is in line with the acidity measurements performed on the same clays in gas phase: cyclohexylamine adsorption-desorption in gas phase showed a decrease in the overall acidity when the activation severity increases.<sup>32</sup> On the contrary, aluminium exchange leads to the formation of acid sites, due to enhanced polarization of water molecules in the primary coordination sphere Al<sup>3+</sup> free cations.<sup>33-35</sup> Acid sites titration in water is well correlated with CEC, except for SDN-Na.

Therefore, the pristine SDN-Na clay holds only a few acid sites which are mostly Lewis acid sites. HCl activation or with aluminium exchange creates numerous Brønsted and Lewis sites and this acidity is still effective in water. However, increasing the concentration of HCl during activation led to decrease the number of Brønsted and Lewis acid sites. For oligosaccharides valorisation, Brønsted acid sites are necessary

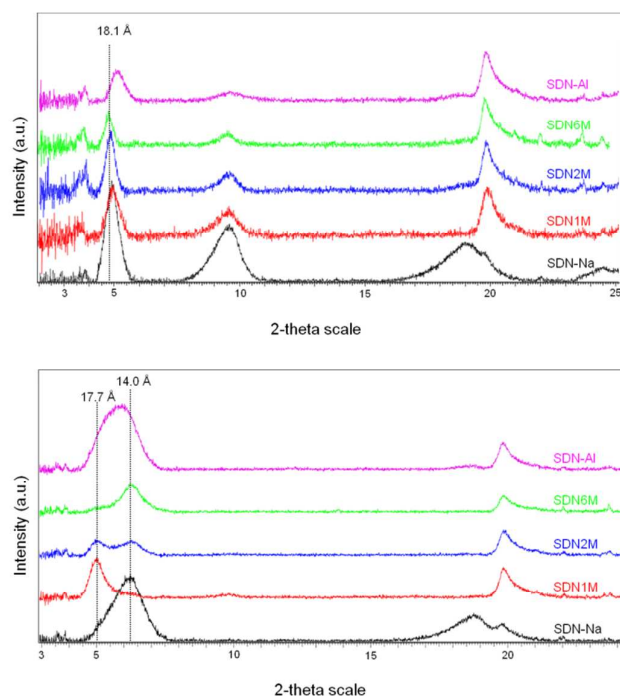


**Figure 2.** a) XRD diffractograms of clay catalysts after glucose, xylose and arabinose adsorption; b) XRD diffractograms of clay catalysts after maltose adsorption. The diffractograms were performed over a glass blade where the clay suspension is deposited and dried at 60°C.

for the hydrolysis reaction<sup>36</sup> even if other Lewis-catalyzed reactions can occur and for example produce carboxylic acid.<sup>37</sup>

### 3.2. Maltose and sugars adsorption capacities

Sugars adsorption on clays was studied at room temperature using in a first step a mixture of three monomer sugars, glucose, xylose and arabinose (GXA, 10 g·L<sup>-1</sup> each).

The clays suspensions in sugars solution were dried on a glass blade without filtration before XRD analysis (Figure 2a). The presence of sugars inside the interlayer space was evidenced by the shift of the d001 peak to the lower angles: in all the samples a spacing of 18 Å (± 0.2 Å) was measured, which corresponds to the stacking of two sugar molecules: the glucose molecular dimension is 3.7 Å<sup>34</sup> and the xylose and arabinose dimensions are assumed to be similar.

In a second step, a maltose solution (30 g·L<sup>-1</sup>) replaced the sugars solution to determine if clays could adsorb in the interlayer space larger molecules such as disaccharides. The XRD diffractograms show some modifications of the interlayer space during the maltose adsorption (Figure 2b). Two peaks are present in the low angles, one corresponding to an interlayer spacing in the range 17.6-17.8 Å and the second to 14 Å. The dimension of the former matches the molecular size of maltose reported in the literature: the molecular dimensions of maltose is 5 Å.<sup>34</sup> The interlayer spacing is here 8 Å, assuming that the tetrahedral-octahedral-tetrahedral (TOT)

sheets have a height of 9.5 Å, which indicates an intercalation of maltose following a double layer arrangement.<sup>35</sup> The second peak corresponds to the hydrated interlayer space, slightly expanded due to the water molecule dimension (1.7 Å).<sup>34</sup> The ratio between the two peaks heights varies with the activation conditions: for SDN1M, it shows that the major part of the interlayer space is occupied by maltose, for SDN2M the maltose-containing interlayer space is equal to the hydrated interlayer space, and for SDN6M the maltose-expanded interlayer space is minor. Interestingly, for SDN-Na, there is only one broad d001 peak, evidencing that maltose adsorption leads only to a slight expansion of the interlayer space, and a peak attributed to amorphous maltose appears around 18.5 °2-theta. For SDN-AI, the d001 peak is broad and high, indicating that maltose adsorption occurs but does not lead to the occupation of the major part of the interlayer space.

Thus, a correlation can be drawn between the adsorption of polar molecules such as sugars and the evolution of the clay structure: in mild activation conditions, the clay structure is preserved and so is the sugars adsorption ability. In harsh activation conditions, the clay structure is partially destroyed and the sugar adsorption capacity is lower. In short, the adsorption of maltose and monomer sugars inside the interlayer space of clays is possible if the clays are activated in mild conditions or after aluminium exchange. The interlayer space represents a wide surface area where acid sites are present. It is thus important that OS can reach these sites to be further hydrolysed. However, after activation in harsh conditions, the maltose ability to adsorb inside the interlayer space is lost, in correlation with the loss of clay structure. One can notice that for acid activated clays, carbohydrate adsorption capacity is correlated with CEC and not with BET surface area, i.e. the adsorption of polar molecules depends on the cation exchange capacity and not on the accessibility of non polar surface area.

### 3.3. Hydrolysis of a model compound: maltose

Maltose is a glucose dimer with  $\alpha$ -(1-4) linkage. It has been chosen as a model compound for soluble OS, preferentially to sucrose which is too reactive, and to cellobiose which is less reactive.<sup>36</sup>

A comparative study was performed between the SDN-Na clay, which is the material from which the activated clays are prepared, the aluminium-exchanged clay (SDN-AI), and the HCl-activated clays. A blank test with maltose in pure water without catalyst was also performed. Figure 3a presents the maltose conversion during the catalytic test for each catalyst. In the absence of clay catalyst, the conversion remained low, fewer than 10 %, over 24 h (data not shown).

The clays can be ordered in three groups. SDN-AI exhibited a low conversion, reaching only 28 % after 24 h, with a linear progress. The HCl-activated clays had similar conversion profile, with a linear conversion curve and a final conversion from 39 % to 43 %, with the ranking SDN1M > SDN6M > SDN2M. However, the SDN2M clay led to a faster conversion

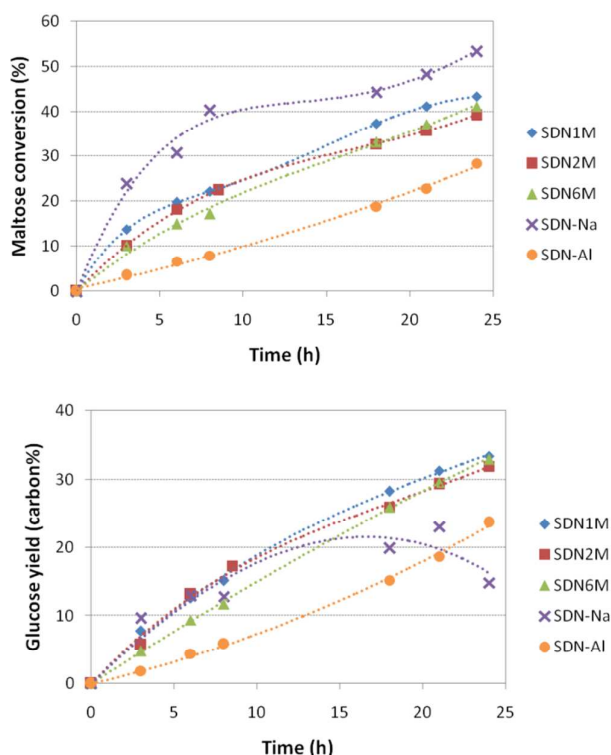


Figure 3. Maltose hydrolysis test over clay catalysts: a) maltose conversion; b) glucose yield. The dotted lines are added for eye guide.

than SDN6M in the first 8 h, probably because of its better sugars adsorption capacity. SD-Na converted maltose in the first 8 h at a high rate, reaching 40 %; the progression was slower during the next 16 h, leading to a 53 % final conversion.

The glucose yield (Figure 3b) was also low for the SDN-AI catalyst, with a 24 %<sub>carbon</sub> final glucose yield. All the HCl-activated clays led to a linear increase of glucose yield during 24 h, ending at 32-33 %<sub>carbon</sub>. No glucose degradation occurred. SD-Na produced an important amount of glucose until 21 h, reaching 24 %<sub>carbon</sub>, but in the last 3 h the glucose yield decreased to 15 %<sub>carbon</sub>, indicating a glucose-consuming reaction. However, the glucose yield was much lower than the maltose conversion and the final carbon balance, calculated from the sum of the products analysed by HPLC-RI (see Table S2 in ESI), is around 65 %<sub>carbon</sub>. The high conversion observed earlier is thus attributed to irreversible maltose adsorption on the SDN-Na clay and to the formation of other products observed by HPLC-UV, among which HMF, a compound known as a glucose dehydration product, with a 0.04 g.L<sup>-1</sup> concentration, i.e. 5.7 %<sub>carbon</sub> yield.

## ARTICLE

Journal Name

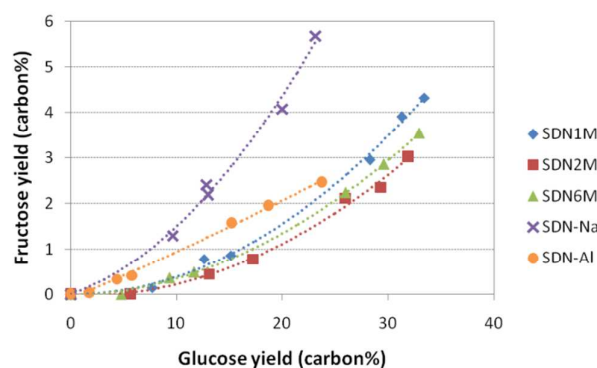


Figure 4. Fructose yield as a function of glucose yield during maltose hydrolysis test over clay catalysts. The dotted lines are added for eye guide.

Besides glucose, fructose, the product of glucose isomerisation, was detected in the reaction medium. The fructose yield was correlated with the glucose yield, as shown on Figure 4.

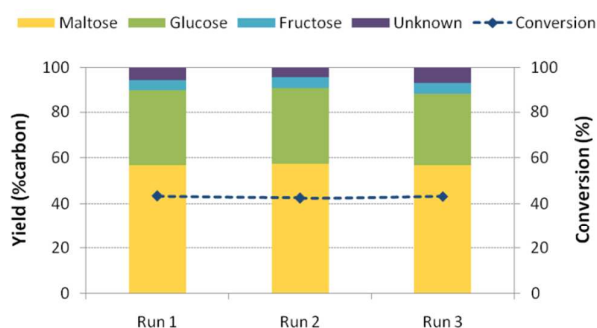
- 5 The nature of the catalyst also modified the fructose production: the SDN-Na and SDN-Al clays tended to produce fructose more easily than the HCl-activated clays, at equivalent glucose yield. In literature, glucose isomerisation into fructose is attributed to basic catalytic sites<sup>37</sup> or to Lewis acid sites<sup>38</sup>
- 10 The presence of Lewis acid sites in both clays was evidenced by FTIR-pyridine adsorption (see part 3.1.). The presence of basic sites on SDN-Na might be possible too.

- From the maltose hydrolysis test, it can be concluded that the SDN-Al catalyst was not as active as expected from the acid sites titration result, and led to a low glucose yield. The SDN-Al clay also catalyses the isomerisation of glucose into fructose. A deactivation of the acid sites is possible, maybe induced by the hydrothermal reaction medium or by carbon deposition on the catalyst. Indeed, the BET surface area measured after test was 95 m<sup>2</sup>·g<sup>-1</sup>, i.e. 32 % lower than the surface of fresh SDN-Al. Aluminium leaching was also evidenced by ICP-OES analysis of the maltose hydrolysis reaction medium (0.8 mg·L<sup>-1</sup> Al detected in aqueous phase).

- The HCl-activated clays gave a good maltose conversion rates with a corresponding glucose yield. Their isomerisation activity is limited. Their difference in acid sites concentration is not high enough to lead to different activities. However, SDN1M exhibits the higher acid sites concentration and the best maltose hydrolysis activity. The SDN2M good adsorption capacity permits a faster maltose conversion in the beginning of the reaction. SDN-Na did not act as an acid catalyst, adsorbing maltose but not giving the corresponding glucose yield and catalysing side reactions such as glucose isomerisation.

### 3.4. Recyclability of SDN1M catalyst during maltose hydrolysis

- The SDN1M clay was submitted to a recyclability test to evaluate its stability in the aqueous reaction medium. The recyclability test consisted in performing three times the maltose hydrolysis test, the catalyst being filtrated and dried overnight at room temperature between two tests. The catalytic performances were stable over three runs (Figure 5):



the conversion and selectivity into glucose are similar after 72 h (third run). Thus, the HCl-activated clays were assumed to be stable in aqueous medium. This is a first step for the design

Figure 5. Maltose conversion and products distribution during three consecutive maltose hydrolysis tests over SDN1M.

of stable hydrolysis catalysts. However, the stability in autohydrolysis liquors is not guaranteed: the low pH, the presence of impurities, the different reactants can also have an impact on the catalyst deactivation.

### 3.5. Oligosaccharides liquor hydrolysis

Table 2 shows the composition of the OS liquor obtained from rice straw autohydrolysis. These liquors mainly contain oligosaccharides (total of 11.6 g·L<sup>-1</sup>) together with lower concentrations of monosaccharides, acetic acid and minor amounts of sugar degradation products (furfural and HMF). The OS present are putatively derived both from the L-arabino-(4-O-methyl-D-glucurono)-D-xylan and easily hydrolyzed glucans present in the rice straw.<sup>39</sup> As such, it is predicted that there may be two main classes of OS, XOS putatively substituted by arabinosyl, acetyl and glucuronic (not measured) groups and GlcOS. Regarding their degree of polymerization (DP), the majority of the OS present in this liquor are mainly large OS. Actually, it can be estimated from previous results<sup>20</sup> that more than half of the OS have an average DP between 54 and 23, 32 % an average DP between 22 and 10 and 15% of the OS have a DP between 3 and 10. XOS are homogeneously distributed among DP. Conversely, GlcOS are mainly found as larger OS, with a DP above 22 accounting for more of 90% of the total GlcOS. Besides OS, monosaccharides (glucose, xylose and arabinose in a total concentration of 3.36 g·L<sup>-1</sup>) and furan derivatives (0.35 g·L<sup>-1</sup>) are also present as well as acetic acid, and phenolic compounds. Furthermore, other components such as proteins or amino acids may also be present together with some biomass derived salts (not measured) and phenolic compounds (slightly above 2 g·L<sup>-1</sup>, data not shown).

**Table 2** Composition of the liquors obtained from autohydrolysis of rice straw (log  $R_0=4.15$ )

Compound	Concentration (g.L <sup>-1</sup> )
Gluco-oligosaccharides <sup>a</sup>	3.38
Xylo-oligosaccharides <sup>a</sup>	7.34
Arabino-oligosaccharides <sup>a</sup>	0.90
Acetyl groups	0.48
Glucose	0.99
Xylose	1.89
Arabinose	0.83
Acetic acid	0.88
HMF	0.13
Furfural	0.19
Total OS	11.61

<sup>a</sup> Values obtained with the post-hydrolysis method.

The hydrolysis of the OS-containing liquor was performed over the SDN1M clay catalyst, at 120°C, during 24 h. Figure 6a compares the composition of the fresh OS-rich liquor with the results obtained after 24 h at 120°C without any catalyst (blank) and in the presence of the SDN1M clay (SDN1M). The results are presented as sugars, acetic acid, and furans concentrations. After 24 h at 120°C in the absence of any catalyst, the liquor composition did not change much. The xylose concentration increases from 1.9 to 2.3 g.L<sup>-1</sup> and small increases in furfural and acetic concentrations were observed, showing a high stability of rice-straw OS.

In the presence of the SDN1M clay catalyst, the glucose, xylose, arabinose and acetic acid concentrations clearly surpassed the values obtained without catalyst, whereas the furfural and HMF concentrations remained unchanged with without clay catalyst. This is the evidence of a selective catalytic hydrolysis of OS leading to the corresponding monosaccharides and acetic acid. From this test it is obvious that the sugars degradation into HMF and furfural is not catalysed by the SDN1M clay in the studied conditions, conversely to what would happen when using a mineral acid such as sulphuric acid.

The post-hydrolysis treatment is assumed to completely hydrolyse the OS present in the liquor and thus gives an estimation of the maximum sugars concentrations that can be reached. In the presence of the clay catalyst, the increase in glucose and xylose concentrations represent 15 % of the yield obtained by post-hydrolysis, whereas the increase in arabinose and acetic acid concentrations represent respectively 48 % and 72 % of the maximum concentration obtained by post-hydrolysis (Figure 6b).

SDN1M led to a partial hydrolysis of OS. Arabinose, which constitutes side units of XOS, was easily and almost completely depolymerised, as well as acetyl groups, whereas skeleton units such as xylose were only partially hydrolysed and remain as monomers and oligomers after the reaction. Thus, the catalytic hydrolysis led to trim the XOS present in the rice-straw hydrolysate. It is important to remind that the oligosaccharides and disaccharides were not analysed. Consequently, the decrease in polymerisation degree caused by cleavages of glycosidic bonds localised in the middle of the

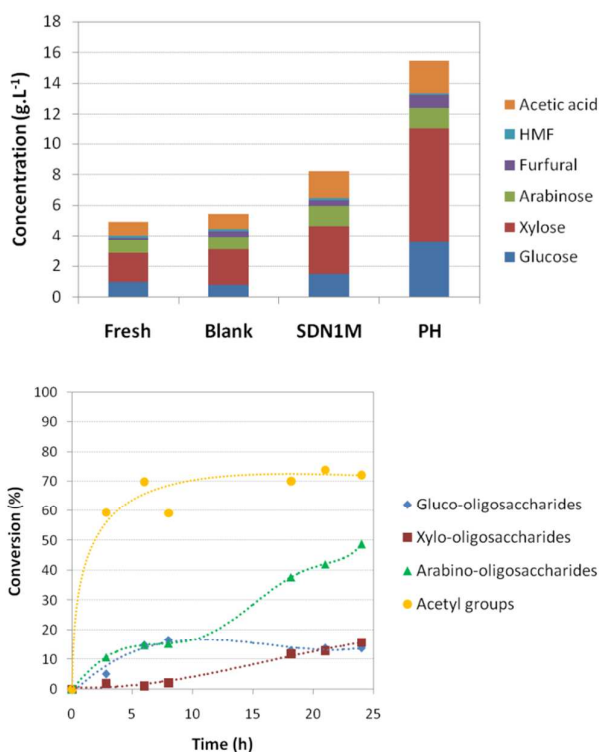


Figure 6. a) Oligosaccharides-rich liquor composition; fresh, after 24 h at 120°C without catalyst (Blank) and after 24 h in the presence of SDN1M clay catalyst (SDN1M); b) Hydrolysis of OS-rich liquor over SDN1M clay: conversion of oligosaccharides and acetyl groups. The dotted lines are added for eye guide.

sugars chain was not detected. A significant part of the potential hydrolytic activity of the clay might thus remain imperceptible in these conditions.

The sugars concentration change during the test is presented in Figure 6, together with HMF, furfural and acetic acid concentrations. During the first 8 h of the test, the conversion of XOS was very low whereas the GlcOS conversion and arabinose production increased until 17 % and 15 %, respectively. From 8 h to 24 h, GlcOS conversion did not increase anymore whereas the AOS conversion increased from 15 % to 49 % and the XOS from 2 % to 16 %. Besides, the concentration of HMF was stable (0.15 g.L<sup>-1</sup>) and the increase in furfural concentration was limited (from 0.21 to 0.38 g.L<sup>-1</sup>) indicating that the glucose was not dehydrated and that the pentoses dehydration into furfural was slow. The acetyl groups conversion was almost linear, reaching 72 % after 24 h. Thus, the OS hydrolysis took place as follows: first, the small GlcOS are hydrolysed quickly into glucose and the side groups of ex-hemicellulose OS, arabinose and acetyl groups, are hydrolysed too. Secondly, the main chain groups, xylose units were deconstructed after 18 h. The dehydration of xylose and arabinose into furfural occurred but was very limited.

Finally, the suitability of clay catalysts for selective OS hydrolysis is demonstrated: the selective production of glucose and arabinose is obtained, as well as the trimming of XOS. This method is under improvement for high DP oligosaccharides as



## ARTICLE

## Journal Name

the ones used in this study but it is suitable for low DP oligosaccharides.

#### 4. Conclusions

Porto Santo montmorillonite clays were investigated as catalysts for the hydrolysis of OS. It was shown that the activation method determines the structure properties and acidity of the clay catalyst. HCl-activated clays are more efficient for the hydrolysis reaction in water than Al-exchanged clay and are able to hydrolyse OS-rich liquor, leading to simple XOS by removing side groups such as arabinosyl and acetyl groups. The degradation reactions are limited. However, the production of monomer sugars from OS is low when compared to mineral acid catalysis. In a near future, clays with improved acidity will be designed to improve the hydrolysis performances.

#### Acknowledgements

The authors thank Ivone Torrado (LNEG), Duarte Correia and Joana Pereira (LREC) for their technical help. Francis Bougie and IRCÉLYON are acknowledged for the kind assistance in BET analyses. This work was supported by FEDER (Programa Operacional Factores de Competitividade–COMPETE) and Portuguese funds (FCT - Fundação para a Ciência e a Tecnologia, projects PTDC/AGR-ALI/122261/2010, PTDC/CTM-CER/1121295/2010 and PEst-OE/QUI/UI0674/2011).

1. F. M. Girio, C. Fonseca, F. Carvalheiro, L. C. Duarte, S. Marques and R. Bogel-Lukasik, *Bioresour. Technol.*, 2010, **101**, 4775-4800.
2. A. Fuente-Hernández, P.-O. Corcos, R. Beauchet and J.-M. Lavoie, in *Liquid, Gaseous and Solid Biofuels - Conversion Techniques*, ed. P. Z. Fang, InTech, Editon edn., 2013.
3. F. Carvalheiro, G. Garrote, J. C. Parajó, H. Pereira and F. M. Girio, *Biotechnol. Progr.*, 2005, **21**, 233-243.
4. L. C. Duarte, T. Silva-Fernandes, F. Carvalheiro and F. M. Girio, *Appl. Biochem. Biotechnol.*, 2009, **153**, 116-126.
5. P. i. Mäki-Arvela, T. Salmi, B. Holmbom, S. Willför and D. Y. Murzin, *Chem. Rev.*, 2011, **111**, 5638-5666.
6. A. Moure, P. Gullón, H. Domínguez and J. C. Parajó, *Process Biochem.*, 2006, **41**, 1913-1923.
7. M. J. Vázquez, J. L. Alonso, H. Domínguez and J. C. Parajó, *Trends Food Sci. Technol.*, 2000, **11**, 387-393.
8. L. Vilcocq, P. C. Castilho, F. Carvalheiro and L. C. Duarte, *ChemSusChem*, 2014, **7**, 1010-1019.
9. Y. Kim, R. Hendrickson, N. Mosier and M. R. Ladisch, *Energy & Fuels*, 2005, **19**, 2189-2200.
10. J. A. Bootsma, M. Entorf, J. Eder and B. H. Shanks, *Bioresour. Technol.*, 2008, **99**, 5226-5231.
11. F. Guo, Z. Fang, C. C. Xu and R. L. Smith, Jr., *Prog. Energy Combust. Sci.*, 2012, **38**, 672-690.

12. M. Kitano, D. Yamaguchi, S. Suganuma, K. Nakajima, H. Kato, S. Hayashi and M. Hara, *Langmuir*, 2009, **25**, 5068-5075.
13. C. E. Fernandes, PhD thesis, Universidade da Madeira, 2007.
14. M. Caine, G. Dyer, I. Holder, B. N. Osborne, W. A. Matear, R. W. McCabe, D. Mobbs, S. Richardson and L. Wang, in *Natural Microporous Materials in Environmental Technology*, eds. P. Misaelides, F. Macásek, T. J. Pinnavaia and C. Colella, Springer Netherlands, Editon edn., 1999, pp. 49-69.
15. C. H. Zhou, *Appl. Clay Sci.*, 2011, **53**, 87-96.
16. A. Vaccari, *Appl. Clay Sci.*, 1999, **14**, 161-198.
17. D. S. Tong, X. Xia, X. P. Luo, L. M. Wu, C. X. Lin, W. H. Yu, C. H. Zhou and Z. K. Zhong, *Appl. Clay Sci.*, 2013, **74**, 147-153.
18. P. L. Dhepe and R. Sahu, *Green Chem.*, 2010, **12**, 2153-2156.
19. R. Sahu and P. L. Dhepe, *ChemSusChem*, 2012, **5**, 751-761.
20. P. Moniz, H. Pereira, L. C. Duarte and F. Carvalheiro, *Industrial Crops and Products*, 2014, **62**, 460-465.
21. P. Moniz, J. Lino, L. C. Duarte, L. B. Roseiro, C. G. Boeriu, H. Pereira and F. Carvalheiro, 2014, **submitted**.
22. C. Catrinescu, C. Fernandes, P. Castilho and C. Breen, *Applied Catalysis A-General*, 2006, **311**, 172-184.
23. L. Ammann, F. Bergaya and G. Lagaly, *Clay Minerals*, 2005, **40**, 441-453.
24. C. A. Emeis, *Journal of Catalysis*, 1993, **141**, 347-354.
25. M. Guisnet, P. Ayrault, C. Coutanceau, M. Fernanda Alvarez and J. Datka, *Journal of the Chemical Society, Faraday Transactions*, 1997, **93**, 1661-1665.
26. A. Onda, T. Ochi and K. Yanagisawa, *Green Chem.*, 2008, **10**, 1033-1037.
27. A. Sluiter, B. Hames, R. Ruiz, C. Scarlata, J. Sluiter and D. Templeton, *National Renewable Energy Laboratory, Golden, CO*, 2006.
28. K. Okada, N. Arimitsu, Y. Kameshima, A. Nakajima and K. J. D. MacKenzie, *Appl. Clay Sci.*, 2006, **31**, 185-193.
29. S. Brunauer, P. H. Emmett and E. Teller, *J. Am. Chem. Soc.*, 1938, **60**, 309-319.
30. G. Chen, J. Pan, B. Han and H. Yan, *J. Dispersion Sci. Technol.*, 1999, **20**, 1179-1187.
31. P. Komadel, *Clay Minerals*, 2003, **38**, 127-138.
32. C. Fernandes, C. Catrinescu, P. Castilho, P. A. Russo, M. R. Carrott and C. Breen, *Applied Catalysis a-General*, 2007, **318**, 108-120.
33. M. P. Atkins, D. J. H. Smith and D. J. Westlake, *Clay Minerals*, 1983, **18**, 423-429.
34. R. Gregory, D. J. H. Smith and D. J. Westlake, *Clay Minerals*, 1983, **18**, 431-435.
35. D. T. B. Tennakoon, R. Schlögl, T. Rayment, J. Klinowski, W. Jones and J. M. Thomas, *Clay Minerals*, 1983, **18**, 357-371.
36. R. Kourieh, S. Bennici, M. Marzo, A. Gervasini and A. Auroux, *Catal. Commun.*, 2012, **19**, 119-126.

Journal Name

ARTICLE

38 37. F. Chambon, F. Rataboul, C. Pinel, A. Cabiach, E. Guillon and N. Essayem, *Applied Catalysis B-Environmental*, 2011, **105**, 171-181.

Catalysis Science & Technology Accepted Manuscript